Neutron detection in the frame of spatial magnetic spin resonance

AUTHOR(S):

Jericha, Erwin; Bosina, Joachim; Geltenbort, Peter; Hino, Masahiro; Mach, Wilfried; Oda, Tatsuro; Badurek, Gerald

CITATION:

Jericha, Erwin ...[et al]. Neutron detection in the frame of spatial magnetic spin resonance. Nuclear Instruments and Methods in Physics Research, Section A: Accelerators, Spectrometers, Detectors and Associated Equipment 2016, 845: 552-555

ISSUE DATE:

2016

URL:

http://hdl.handle.net/2433/216199

Nuclear Instruments and Methods in Physics Research A 845 (2017) 552–555

Contents lists available at ScienceDirect

Nuclear Instruments and Methods in Physics Research A

journal homepage: www.elsevier.com/locate/nima

Neutron detection in the frame of spatial magnetic spin resonance

Erwin Jericha [a,*], Joachim Bosina [a,b,c], Peter Geltenbort [c], Masahiro Hino [d], Wilfried Mach [a], Tatsuro Oda [e], Gerald Badurek [a]

[a] TU Wien, Atominstitut, Stadionallee 2, 1020 Wien, Austria
[b] Austrian Academy of Sciences, Stefan Meyer Institute, Boltzmanngasse 3, 1090 Wien, Austria
[c] Institut Laue–Langevin, 71 Avenue des Martyrs, 38042 Grenoble, France
[d] Kyoto University, Research Reactor Institute, Kumatori, Osaka 590-0494, Japan
[e] Kyoto University, Department of Nuclear Engineering, Kyoto 615-8540, Japan

ARTICLE INFO

Article history:
Received 15 March 2016
Accepted 29 April 2016
Available online 30 April 2016

Keywords:
Neutron detection
Neutron time-of-flight
Polarized neutrons
Spatial magnetic spin resonance
Spin flipper

ABSTRACT

This work is related to neutron detection in the context of the polarised neutron optics technique of spatial magnetic spin resonance. By this technique neutron beams may be tailored in their spectral distribution and temporal structure. We have performed experiments with very cold neutrons (VCN) at the high-flux research reactor of the Institut Laue Langevin (ILL) in Grenoble to demonstrate the potential of this method. A combination of spatially and temporally resolving neutron detection allowed us to characterize a prototype neutron resonator. With this detector we were able to record neutron time-of-flight spectra, assess and minimise neutron background and provide for normalisation of the spectra owing to variations in reactor power and ambient conditions at the same time.

1. Introduction

The development of spatial magnetic spin resonance dates back to the 1960s. Its first experimental realisation was reported in 1968 [1]. There it was found that a magnetic field configuration consisting of a periodic spatially alternating static resonator field B_1 and a static homogeneous selector field B_0 orthogonal to B_1 changes the polarisation of a neutron beam as a function of neutron wavelength λ. Resonance conditions for the wavelength, $\lambda = \lambda_0$, and the amplitude of B_1 may be formulated for a given selector field B_0, [2,3]. The present project has been motivated by the concurrent development of the neutron decay instrument PERC which relies on a pulsed polarised cold neutron beam with defined spectral properties [4,5]. Letting a polarised neutron beam pass our resonator, we obtain at its exit a neutron beam which has inverted polarisation for neutrons with wavelength distributed around the resonance wavelength λ_0. When the neutron beam passes additionally through a broadband spin flipper like a current sheet that inverts the polarisation of the neutron beam as a whole, only the monochromatic distribution of resonant neutrons is polarised in the initial direction, afterwards. If we place now a polarisation analyser in the beam path only these resonantly flipped neutrons will be transmitted. Therefore a setup consisting of polariser, resonator, broadband spinflipper and analyser will act as a monochromator for polarised neutron beams which may also be pulsed with an appropriate operation mode of the resonator. A corresponding experimental setup is shown in Fig. 1.

In recent years we have developed resonators with independent elements which allow us to tailor the neutron beam with high flexibility. The principal scheme was introduced in [6], and several prototypes were designed [3] and constructed [7]. First experiments were then performed at a dichromatic thermal neutron beam at the TRIGA reactor of the Atominstitut in Vienna [7,8]. First experiments at a polychromatic *white* neutron beam were performed recently with very cold neutrons (VCN) at the instrument PF2/VCN at ILL. These slow neutrons are ideal for tests with relaxed conditions on resonator field strength and resonator timing.

2. Experiments

At ILL, VCN are extracted from the vertical cold neutron source via a bent vertical neutron guide and enter a cabin dedicated for VCN experiments. At the entrance to the experimental setup a disc chopper is placed. It consists of an aluminum disc covered with a Gd layer that absorbs VCN with perfect efficiency. The chopper is typically operated with 10 Hz repetition rate. Neutrons pass the disc through an open window. After the chopper the neutrons enter a 2.2 m large aluminum box where the neutron optical components are mounted. Immediately after the exit window the neutron detector is placed.

* Corresponding author.
E-mail address: jericha@ati.ac.at (E. Jericha).
URL: http://www.ati.ac.at (E. Jericha).

http://dx.doi.org/10.1016/j.nima.2016.04.103

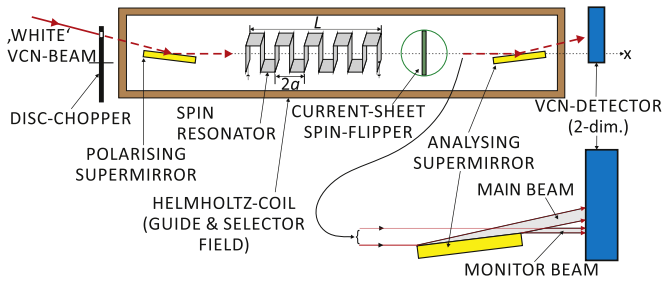

Fig. 1. Experimental setup for the neutron resonator at the VCN beam line at ILL. Neutron pass from the curved neutron guide through a disc chopper opening into an aluminum box which may be flooded with helium. Inside the box are located a polarising supermirror, the multi-element resonator, a broadband current-sheet spin flipper, and an analysing supermirror. Outside the box the position-sensitive neutron detector is placed close to the exit window. At the analyser the exiting neutron beam is divided into a main beam and a monitor beam used for reference purposes.

Table 1
Technical specifications of the BIDIM26 detector used in the VCN experiment [9].

Detecting element	Multi Wire Proportional Chamber (MWPC)
Position measurement	Individual wires readout
Active area	26×26 cm^2
Position resolution	2×2 mm^2
Window thickness	4 mm
Conversion gap thickness	3 cm
Gas mixture	500 mbar ^{3}He + 1.5 bar CF_4
Global count rate	$\sim 2 \times 10^5$/s

The surfaces of the supermirror polarisers are aligned at an angle of about 9° with respect to the incoming neutron beam. The footprint of a beam of width w impinging on a surface under an angle θ has a length $\Delta l = w/\sin\theta$. For $w = 15$ mm and $\theta = 9°$, we obtain $\Delta l = 96$ mm, larger than the 75 mm diameter of the supermirror. Therefore we can use the portion of the beam which does not hit the analysing supermirror for monitoring purposes. Such a monitor beam offers some distinct advantages: it is derived from the same incident flux as the main beam, has the same path length through gas atmosphere and resonator sheets as the main beam, it is reflected from the polariser and guarantees therefore normalisation on the same initial polarisation, it is independent on manipulation of beam polarisation throughout the setup because it bypasses the analyser.

Experiments were carried out as integral measurements or time-of-flight spectra which give us access to the spectral behaviour. They are produced either by the rotating disc chopper or the pulsed neutron resonator or a combination of both. The TOF start signal is generated by either by the chopper or by the resonator, in case the chopper is at rest in open position. In recording the neutron intensity for the various settings, the VCN detector is a key component of the experimental setup. Its specifications are given in Table 1 according to [9]. The detector itself can be operated in different modes owing to a versatile data acquisition electronics attached to it. In the most general case, each detector element consists of a spatial pixel at coordinate (y_i, z_j) and of size $2\Delta y \times 2\Delta z$ and a time channel t_l of width $2\Delta t$. The neutron counts in this element $N_{ijlm} = N_m(y_i, z_j, t_l)$ in a single time frame m (corresponding to one revolution of the chopper) are given by

$$N_{ijlm} = \int_{y_i-\Delta y}^{y_i+\Delta y} \mathrm{d}y \int_{z_j-\Delta z}^{z_j+\Delta z} \mathrm{d}z \int_{t_l-\Delta t}^{t_l+\Delta t} N_m(y, z, t)\,\mathrm{d}t \tag{1}$$

and a complete measurement of M time frames by

$$N_{ijl} = \sum_{m=1}^{M} N_{ijlm}. \tag{2}$$

Position resolved detector data for two different time channels $t_l \pm \Delta t$ are shown in Fig. 2. The data represent the incoming neutron spectrum passing the disc chopper when its rotates with 10 Hz repetition rate. The counts correspond to about $M = 18{,}000$ time frames. From these neutron counts we may derive position integrated time-of-flight spectra

$$N_l(i_1, i_2, j_1, j_2) = \sum_{i=i_1}^{i_2} \sum_{j=j_1}^{j_2} N_{ijl} \tag{3}$$

or time integrated 2D intensity maps

$$N_{ij}(l_1, l_2) = \sum_{l=l_1}^{l_2} N_{ijl}. \tag{4}$$

Two such intensity distributions are shown in Fig. 3.

3. Discussion

Fig. 3 a illustrates a particular feature about VCN which appear both as directed beam and multi-directional gas at the same time.

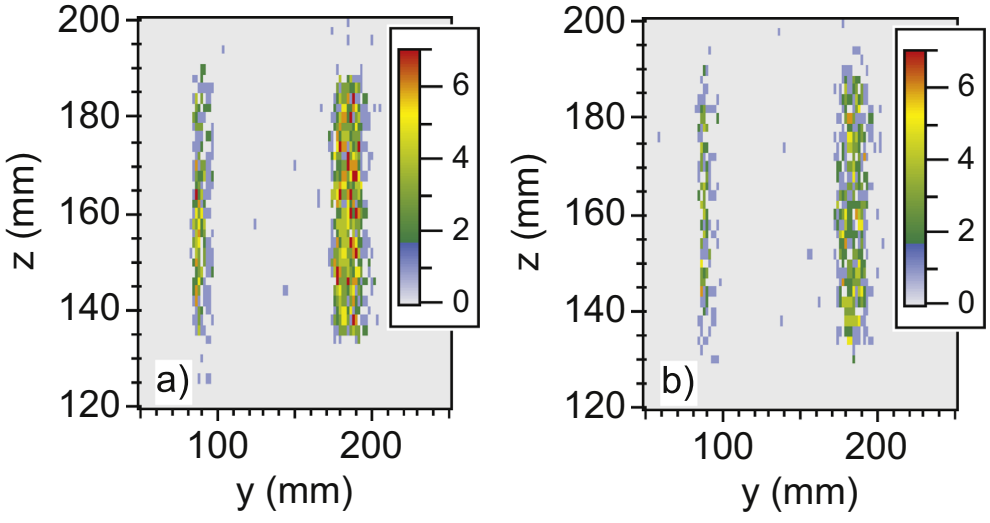

Fig. 2. Time- and position-resolved detector data N_{ijl} with $\Delta x = \Delta y = 1$ mm and $\Delta t = 50$ μs; (a) $t_l = 32.05$ ms ($l = 321$) and (b) $t_l = 40.05$ ms ($l = 401$).

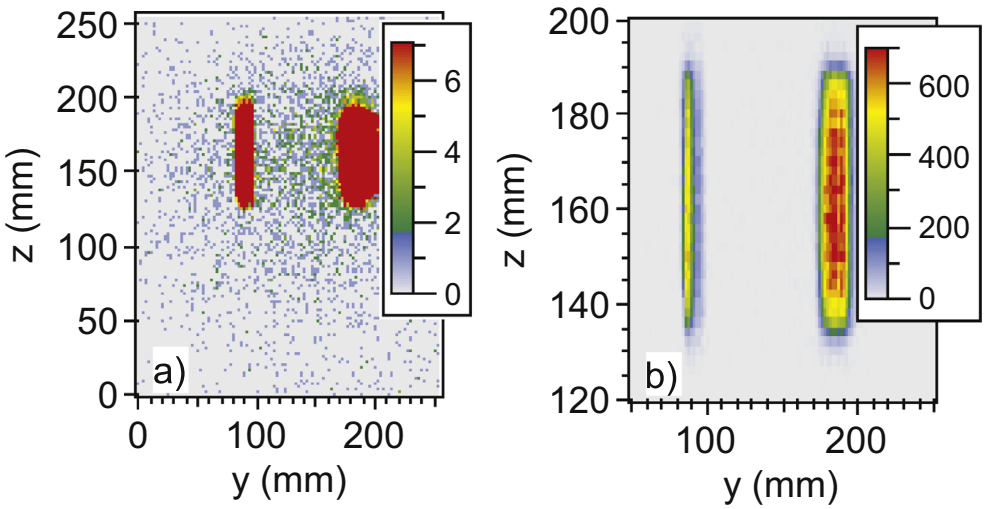

Fig. 3. Time integrated 2D intensity maps $N_{ij}(1, 1000)$ over 1000 time channels, where two of them are shown in Fig. 2. In (a) the full detector area is shown and the intensity scale highlights the background events, in (b) the regions of interest (ROI) with the main beam on the right side and the monitor beam on the left side are seen.

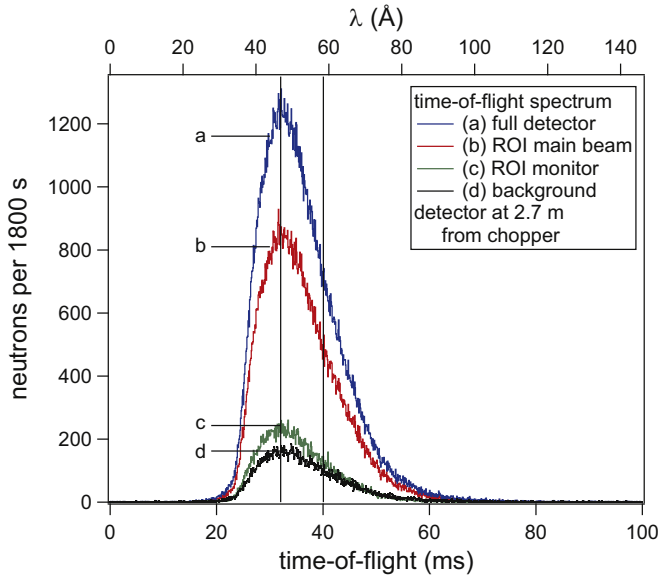

Fig. 4. Neutron TOF spectrum $N_l(i_1, i_2, j_1, j_2)$ of the incident beam, $l_1 = 1$, $l_2 = 1000$ (100 ms): area integrated in (a) over the full detector, $i_1 = j_1 = 1$, $i_2 = j_2 = 128$; (b) over the ROI (20×58 mm^2) for the main beam, $i_1 = 88$, $i_2 = 97$, $j_1 = 67$, $j_2 = 95$; (c) over the monitor beam ROI (8×58 mm^2), $i_1 = 42$, $i_2 = 45$, $j_1 = 67$, $j_2 = 95$; (d) over the full detector minus the two ROIs shown in (b) and (c). The two vertical lines mark the position of the two time slices (see Fig. 2) from which the corresponding data points are calculated.

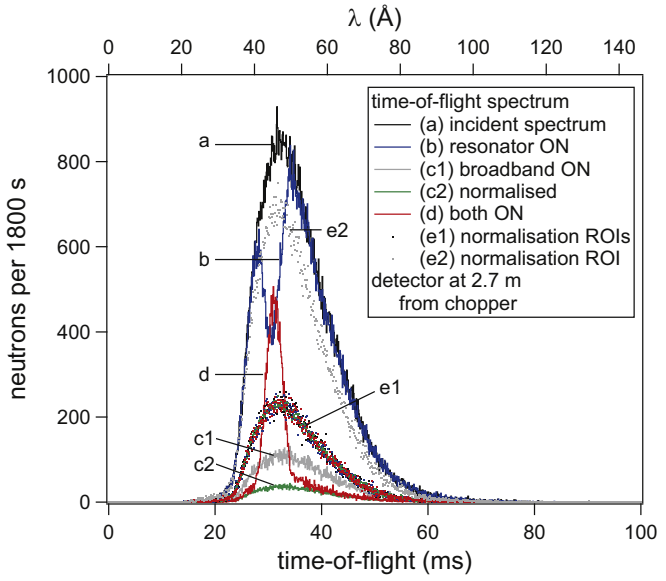

Fig. 5. Neutron TOF spectra taken in 1800 s measurement time: (a) main ROI of the incident beam, this curve corresponds to curve (b) in Fig. 4, (b) ROI of the main beam where the neutron resonator is switched on, (c) ROI of the main beam when the current-sheet is turned on, (c1) intensity after 5400 s measurement time, (c2) rescaled to 1800 s measurement time, (d) main ROI of the beam when both resonator and current-sheet are switched on, (e) monitor ROIs, (e1) for (a)–(d) with 1800 s measurement time, these curves correspond to curve (c) in Fig. 4, (e2) for curve (c1) with 5400 s measurement time, these data are used to normalise the (c1) data.

We see clearly the regions corresponding to the main and monitor beam, respectively. In between and around these regions a neutron background is distributed almost randomly. In Fig. 3 the total counts measured in 1800 s amount to 203,706 or 113.2 per second. The region of interest for the main beam contains 138,654 counts, or 68%, the monitor ROI 36,413 counts, or 18%, and the background amounts to 28,639 counts, or 14%. This last percentage is indeed appreciable, and position-resolved detection allows us to eliminate this background unambiguously. The ROIs used are specified in the caption of Fig. 4.

Use of the monitor beam allows us to take variations in polarisation, fluctuations of the neutron source and variable absorption owing to different environmental conditions into account. Intensity gain or loss can be quantified by a single integral number, namely the number of neutrons reaching the detector per second in the monitor beam ROI. A common normalisation accounts for different measuring times, or number of time frames, employed in measurements which are to be compared. This is illustrated in Fig. 5. Here, the time-of-flight spectra for four different measurements are summarised: (a) the incident spectrum; (b) the spectrum where the resonator is switched on and the resonant neutrons are spin-flipped and therefore cannot pass the analyser into the detector – this can be seen as intensity minimum at the position of the resonant neutrons; (c) the spectrum where the broadband flipper is switched on and practically all neutrons are spin-flipped – in an ideal situation no neutron intensity should be recorded in the detector. Here, the detected intensity is an indicator for the non-ideal polarisation of the neutron beam and labelled as *background*. (c1) shows the actual measurement of 5400 s measuring time which was extended owing to lower

counting statistics with these settings while (c2) was scaled to the common measuring time of 1800 s. (d) the spectrum where both the resonator and the current-sheet spin-flipper are switched on – only the resonant neutrons have the 'right' polarisation at the analyser and would pass the analyser in the ideal case. As an indicator of the non-ideal polarisation the resonant neutron distribution sits of top of the background (c).

Our monitor beam allows us to assess the stability of the neutron source and the experimental setup. For the data shown in Fig. 5 we find an average monitor count rate of 36,284(78) per 1800 s or 20.158(43)/s. The monitor count rates for our four measurements are 20.23(11)/s for (a), 20.11(11)/s for (b), 20.168 (61)/s for (c), and 20.10(11)/s for (d). From these values we find that the neutron source as well as the experimental setup were extremely stable during the measurements (a)–(d). This is also expressed by the fact that the spectra (a) and (b) lie on top of each other, except for the resonant dip, from which we can conclude that the resonator indeed influences the neutrons in a narrow spectral range only, or curves (c2) and (d), from which we can conclude that the resonator is operating properly and that the distribution of resonant neutron sits on the same background that is present when the resonator is switched off. The determination of this *polarisation background* underlines the value of using the position-sensitive detector to discriminate against the background events taking place outside our regions of interest. In measurement (c) 59.2% of the events take place in the monitor ROI, 10.4% in the main beam ROI, and 30.4% occur in the rest of the detector area. Without the possibility to define regions of interest the data quality of this key quantity would be significantly impaired.

Acknowledgement

We gratefully acknowledge that the project has been supported by Deutsche Forschungsgemeinschaft (SPP 1491, Project JE 595/2–1, PREPERC) and the Austrian Fonds zur Förderung der wissenschaftlichen Forschung (Project no. I 528-N20, MONOPOL).

References

[1] G. Drabkin, V. Trunov, V. Runov, Static magnetic field analysis of a polarized neutron spectrum, Sov. Phys. JETP 27 (2) (1968) 194–196.
[2] M. Agamalyan, G. Drabkin, V. Sbitnev, Spatial spin resonance of polarized neutrons – a tunable slow neutron filter, Phys. Rep. 168 (5) (1988) 265–303, http://dx.doi.org/10.1016/0370-1573(88)90081-6.
[3] G. Badurek, C. Gösselsberger, E. Jericha, Design of a pulsed spatial neutron magnetic spin resonator, Phys. B 406 (12) (2011) 2458–2462, http://dx.doi.org/10.1016/j.physb.2010.09.023.
[4] D. Dubbers, H. Abele, S. Baeßler, B. Märkisch, M. Schumann, T. Soldner, O. Zimmer, A clean, bright, and versatile source of neutron decay products, Nucl. Instrum. Methods Phys. Res. A 596 (2) (2008) 238–247, http://dx.doi.org/10.1016/j.nima.2008.07.157.
[5] C. Gösselsberger, H. Abele, G. Badurek, E. Jericha, S. Nowak, G. Wautischer, A. Welzl, Design of a novel pulsed spin resonator for the beta-decay experiment perc, Phys. Proc. 17 (2011) 62–68, http://dx.doi.org/10.1016/j.phpro.2011.06.018.
[6] G. Badurek, E. Jericha, Upon the versatility of spatial neutron magnetic spin resonance, Phys. B 335 (1–4) (2003) 215–218, http://dx.doi.org/10.1016/S0921-4526(03)00240-0.
[7] C. Gösselsberger, H. Abele, G. Badurek, E. Jericha, W. Mach, S. Nowak, T. Rechberger, Neutron beam tailoring by means of a novel pulsed spatial magnetic spin resonator, J. Phys.: Conf. Ser. 340 (2012) 012028–1–8, http://dx.doi.org/10.1088/1742-6596/340/1/012028.
[8] C. Gösselsberger, M. Bacak, T. Gerstmayr, S. Gumpenberger, A. Hawlik, B. Hinterleitner, E. Jericha, S. Nowak, A. Welzl, G. Badurek, Wavelength-selected neutron pulses formed by a spatial magnetic neutron spin resonator, Phys. Proc. 42 (2013) 106–115, http://dx.doi.org/10.1016/j.phpro.2013.03.182.
[9] G. Manzin, Bidim80 and Bidim26 for UCN, Technical Specifications, Technical Report, ILL, 2011.